Macroscopic Spinning Chirality Memorized in Spin-Coated Films of Spatially Designed Dendritic Zinc Porphyrin *J*-Aggregates[**]

*Tatsuya Yamaguchi, Tatsumi Kimura, Hiro Matsuda, and Takuzo Aida**

The breaking of chiral symmetry can occur under nonequilibrated conditions.[1–4] Such a spontaneous induction of optical activity from achiral entities has attracted much attention in relation to the origin of chirality in nature. Representative examples can be seen in growth processes of large electrostatic assemblies of achiral chromophoric compounds such as cyanine dyes and porphyrin derivatives in aqueous media.[5] In these cases, the assemblies are considered to adopt helical architectures, where either the *P* or *M* form is selected only accidentally at the initial stage of the self-organization event and develops predominantly in the subsequent stage. Hence, handedness of emerging chirality is unpredictable. Ribó et al.[5c] have discovered, through studies on electrostatic *J*-aggregation of a 4-sulfonatophenylporphyrin in aqueous media, that the sense of such an optical activity can be selected by the spinning direction of vortex stirring initially applied to the solutions. Herein we report an interesting finding that spin-coated films of dendritic zinc porphyrin *J*-aggregates chiroptically memorize the spinning directions. The optical activities of the spin-coated films are thermally stable and preserved up to the melting temperatures of the *J*-aggregates. In contrast with the previous examples,[5] the *J*-aggregates are optically inactive in solution.

Porphyrin *J*-aggregates have attracted attention because of their potential application as nonlinear optical materials.[6] Although several examples of porphyrin *J*-aggregates have been reported, they are formed mostly in aqueous media;[5b,c] however, there are few examples of *J*-aggregation in organic media[7] which occur because of rather weak π-stacking interactions. We found that zinc porphyrins bearing carboxylic acid (-CO_2H) functionalities at the opposite meso positions undergo supramolecular polymerization by dimerization of the -CO_2H groups to give *J*-aggregates in organic media. The *J*-aggregation takes great advantage of a multi-

---

[*] Dr. T. Yamaguchi, Prof. Dr. T. Aida
Aida Nanospace Project
Exploratory Research for Advanced Technology (ERATO)
Japan Science and Technology Agency (JST)
2-41 Aomi, Koto-ku, Tokyo 135-0064 (Japan)
Fax: (+81) 3-5841-7310
E-mail: aida@macro.t.u-tokyo.ac.jp
Dr. T. Kimura, Dr. H. Matsuda
Photonics Research Institute
National Institute of Advanced Industrial Science and Technology (AIST)
Tsukuba Central 5, 1-1-1 Higashi Tsukuba, Ibaraki 305-8565 (Japan)

[**] T.Y. thanks the JSPS Young Scientist Fellowship.

Supporting information for this article is available on the WWW under http://www.angewandte.org or from the author.

DOI: 10.1002/ange.200461431

point π-stacking interaction between the polymeric zinc porphyrin molecules. Our molecular design strategy also includes introduction of [G2] or [G3] dendritic wedges at the residual two meso positions (**G*m*/*n***$_{\text{acid}}$, where m is the generation number of the dendritic wedges (2 or 3) and n is the number of benzyl ether units (0—2) in the spacer parts of the dendritic wedges; Scheme 1). The dendritic wedges are essential not only for providing the resulting supramolecular polymers with sufficiently high solubilities but also for steric control over the π-stacking interaction among the polymeric focal cores. For comparison, we synthesized a zinc porphyrin dicarboxylic acid (**G0**$_{\text{C18}}$**/1**$_{\text{acid}}$) bearing long alkyl chains, and investigated the aggregation behavior of this nondendritic reference as well as those of ester versions **G*m*/*n***$_{\text{ester}}$, which were the synthetic precursors of **G*m*/*n***$_{\text{acid}}$.

For the synthesis of **G3/1**$_{\text{acid}}$ (Scheme 1), the zinc complex of 5,15-bis(4-methoxycarbonylphenyl)-10,20-bis(4-hydroxyphenyl)porphyrin was treated under alkaline conditions with [G3] poly(benzyl ether) dendron bromide, and the resulting ester (**G3/1**$_{\text{ester}}$) was hydrolyzed with KOH. After neutralization, the reaction mixture was subjected to preparative size-exclusion chromatography (SEC) to isolate **G3/1**$_{\text{acid}}$. Other dendritic zinc porphyrins such as **G2/0**$_{\text{acid}}$–**G2/2**$_{\text{acid}}$, **G3/0**$_{\text{acid}}$, and nondendritic **G0**$_{\text{C18}}$**/1**$_{\text{acid}}$ (Scheme 1) were synthesized in a similar manner to the above and unambiguously characterized.[8] As the benzyl ether spacers between the zinc porphyrin unit and the dendritic wedges become longer, the zinc porphyrin core should possess a larger spatial freedom for the π-stacking interaction (**G2/0**$_{\text{acid}}$ < **G2/1**$_{\text{acid}}$ < **G2/2**$_{\text{acid}}$; **G3/0**$_{\text{acid}}$ < **G3/1**$_{\text{acid}}$). On the other hand, the spatial freedom should become smaller as the dendritic wedges become larger (**G3/0**$_{\text{acid}}$ < **G2/0**$_{\text{acid}}$; **G3/1**$_{\text{acid}}$ < **G2/1**$_{\text{acid}}$). In contrast with the case of these dendritic versions **G*m*/*n***$_{\text{acid}}$, the zinc porphyrin unit in **G0**$_{\text{C18}}$**/1**$_{\text{acid}}$ is omitted because of the absence of dendritic wedges.

We found that [G2] dendritic zinc porphyrin dicarboxylic acids such as **G2/0**$_{\text{acid}}$–**G2/2**$_{\text{acid}}$ all form stable *J*-aggregates in $CHCl_3$. For example, the electronic absorption spectrum of a $CHCl_3$ solution of **G2/2**$_{\text{acid}}$ (5 mM) at 25 °C displayed an intense red-shifted Soret band at 453 nm and a blue-shifted band at 413 nm (Figure 1 c) which is characteristic of zinc porphyrin *J*-aggregates. **G2/1**$_{\text{acid}}$ with shorter benzyl ether spacers exhibited a virtually identical absorption spectral profile to **G2/2**$_{\text{acid}}$ (Figure 1 b). Although **G2/0**$_{\text{acid}}$ without

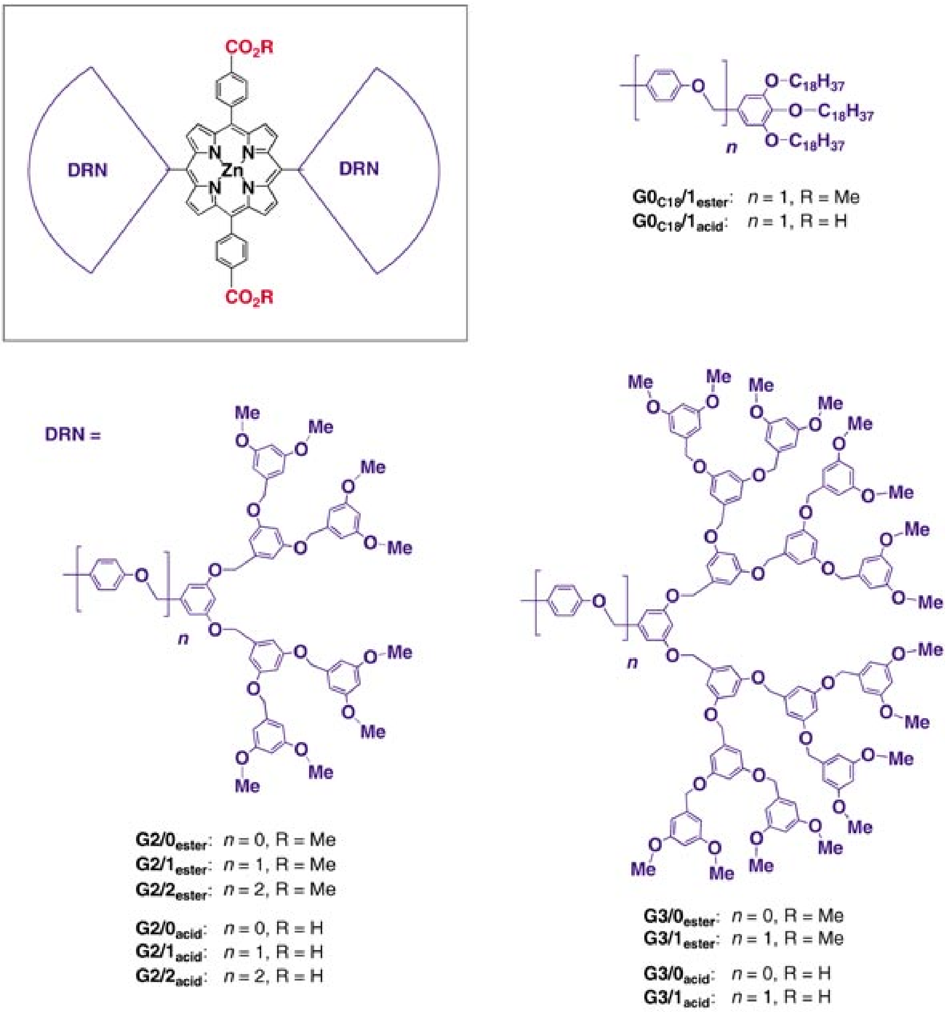

Scheme 1. Structures of the dendritic and nondendritic zinc porphyrin dicarboxylic acids **G*m*/*n***$_{\text{acid}}$ (m = 0, 2, 3, n = 0–2) and their esters **G*m*/*n***$_{\text{ester}}$ (m = 0, 2, 3, n = 0–2).

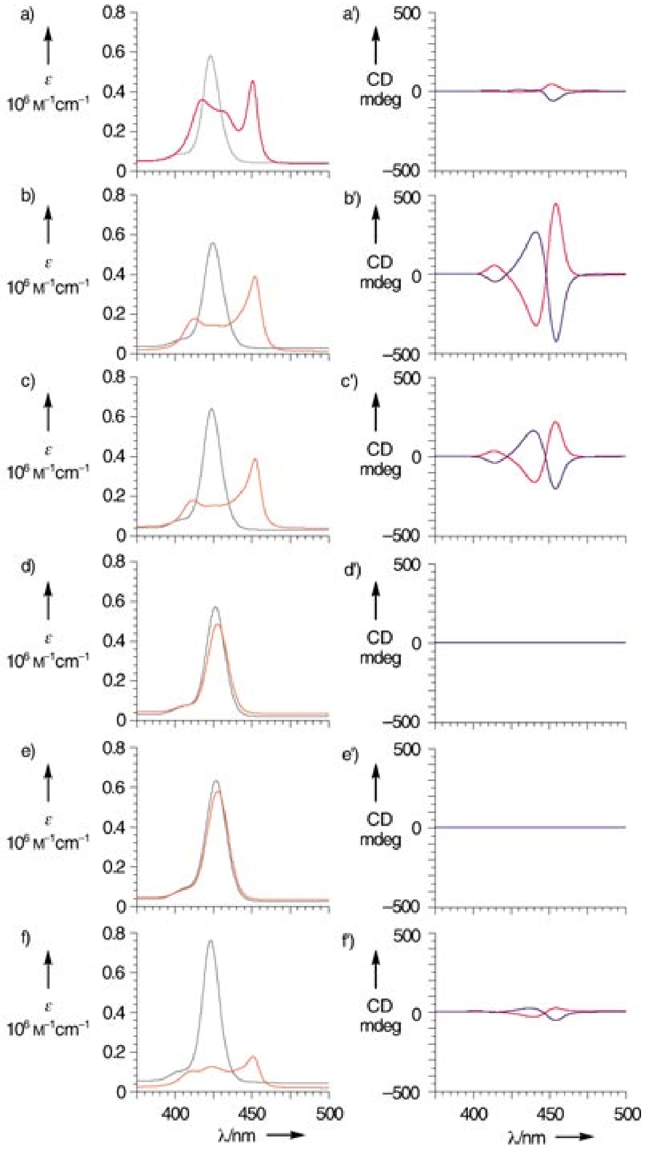

Figure 1. Electronic absorption spectra of solutions (5 mM) of **G*m*/*n***$_{\text{acid}}$ ($m=0$, 2, 3, $n=0$—2; red curves) and **G*m*/*n***$_{\text{ester}}$ ($m=0$, 2, 3, $n=0$—2; green curves) in CHCl$_3$ at 25 °C; a) **G2/0**$_{\text{acid}}$ and **G2/0**$_{\text{ester}}$, b) **G2/1**$_{\text{acid}}$ and **G2/1**$_{\text{ester}}$, c) **G2/2**$_{\text{acid}}$ and **G2/2**$_{\text{ester}}$, d) **G3/0**$_{\text{acid}}$ and **G3/0**$_{\text{ester}}$, e) **G3/1**$_{\text{acid}}$ and **G3/1**$_{\text{ester}}$, and f) **G0**$_{\text{C18}}$**/1**$_{\text{acid}}$ and **G0**$_{\text{C18}}$**/1**$_{\text{ester}}$. CD spectra of thin films of **G*m*/*n***$_{\text{acid}}$ ($m=2$, 3, $n=0$–2) prepared by spin-coating in clockwise (red curves) and counterclockwise (blue curves) spinning directions are also shown; a′) **G2/0**$_{\text{acid}}$, b′) **G2/1**$_{\text{acid}}$, c′) **G2/2**$_{\text{acid}}$, d′) **G3/0**$_{\text{acid}}$, e′) **G3/1**$_{\text{acid}}$, f′) **G0**$_{\text{C18}}$**/1**$_{\text{acid}}$.

benzyl ether spacers formed a *J*-aggregate, it displayed a slightly different absorption spectrum, with two red-shifted Soret bands at 451 and 432 nm (Figure 1 a). The infrared spectra of solutions of **G2/*n***$_{\text{acid}}$ ($n=0$—2; 5 mM) in CHCl$_3$ all showed a carbonyl stretching vibration at 1688 cm^{-1} arising from a dimeric form of CO$_2$H, with only a negligibly small shoulder attributable to free CO$_2$H at 1725 cm^{-1}.[8] Dynamic light scattering (DLS) studies on a dilute solution of *J*-aggregated **G2/1**$_{\text{acid}}$ in CHCl$_3$ (0.05 mM), for example, showed the presence of large assemblies with an average radius of 200 nm.[8] Thus, the zinc porphyrin cores of these dendritic compounds are hydrogen bonded to one another to form supramolecular polymers. In contrast, their ester versions **G2/*n***$_{\text{ester}}$ ($n=0$–2) showed a single Soret band at 423 nm (Figure 1 a–c; green curves), which is characteristic of non-aggregated zinc porphyrins. Therefore, it is concluded that the *J*-aggregation of zinc porphyrins can be induced in organic media by their hydrogen-bonding interactions. We assume that one-dimensional zinc porphyrin polymers formed by the dimerization of the CO$_2$H moieties stack up together, through a multipoint π-electronic interaction, to form a large, two-dimensional (2D) sheetlike assembly (Scheme 2). The difference in the absorption spectral profile between **G2/*n***$_{\text{acid}}$ ($n=1$, 2) and **G2/0**$_{\text{acid}}$ (Figure 1 a–c; red curves) is attributable to a difference in the π-stacking geometry of the zinc porphyrin units. Namely, the *J*-aggregates of **G2/1**$_{\text{acid}}$ and **G2/2**$_{\text{acid}}$ both involve a short, oblique slip of the π-stacked zinc porphyrin units (Scheme 2 a), typical of *J*-aggregated tetraarylporphyrin derivatives, since such a geometry can reduce the steric interference from the meso-aryl groups on the zinc porphyrin units.[9] On the other hand, the *J*-aggregate of **G2/0**$_{\text{acid}}$, which is devoid of any spacers between the dendritic wedges and the zinc porphyrin core, involves a long, non-oblique slip of the π-stacked zinc porphyrin units (Scheme 2 b), possibly because of limited spatial freedom for the π-stacking interaction. The dendritic side chains, which are located presumably on both sides of the 2D sheet, are responsible for the high solubilities of the *J*-aggregates. For reference, the absorption spectral

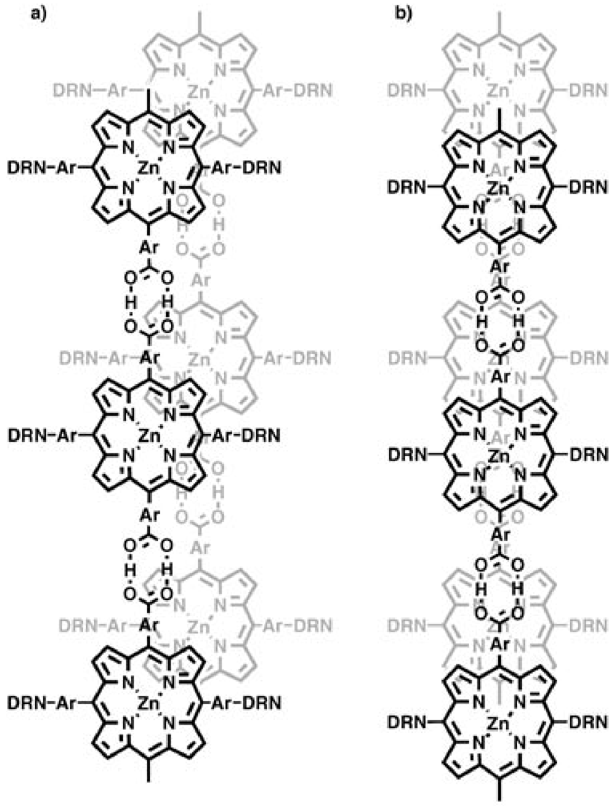

Scheme 2. Structures of zinc porphyrin *J*-aggregates with a short, oblique slip (a) and a long, non-oblique slip (b).

profile of nondendritic **G0$_{C18}$/1$_{acid}$** in hot $CHCl_3$ (Figure 1 f) was analogous to those of *J*-aggregated **G2/1$_{acid}$** and **G2/2$_{acid}$**, but the compound gradually precipitated on standing at 25 °C.

In contrast with the [G2] dendritic zinc porphyrins **G2/*n*$_{acid}$** ($n = 0$–2), solutions of the one-generation higher systems **G3/0$_{acid}$** and **G3/1$_{acid}$** (5 mM) in $CHCl_3$ both displayed a single Soret band at 428 nm, similar to their ester versions, thus indicating that their zinc porphyrin cores are not assembled through π-stacking interactions (Figure 1 d,e). Infrared spectroscopic analysis of these compounds showed a considerable amount of free CO_2H groups at 1725 cm^{-1}, along with dimeric CO_2H groups at 1688 cm^{-1}.[8] Therefore, it is likely that the large dendritic wedges attached to the zinc porphyrin core suppress both the hydrogen-bonding and π-stacking interactions. On the other hand, we also found that **G3/1$_{acid}$** gives a *J*-aggregate in an apolar solvent such as C_6H_6, where a dimeric form of CO_2H is stable. The electronic spectrum of a solution of **G3/1$_{acid}$** in C_6H_6 (5 mM) showed a red-shifted Soret band at 453 nm and a blue-shifted band at 414 nm (Figure 2 b; red curve), whereas ester **G3/1$_{ester}$**, under identical conditions, displayed an ordinary Soret band at 429 nm (Figure 2 b; green curve). Infrared spectroscopic analysis of **G3/1$_{acid}$** in C_6H_6 (5 mM), in contrast with the case in $CHCl_3$, showed a carbonyl stretching vibration predominantly at 1688 cm^{-1} arising from the dimeric form of CO_2H. These observations again support our hypothesis that the zinc porphyrin units, when polymerized through hydrogen-bonding interactions, have an enhanced capability for π stacking. In contrast, **G3/0$_{acid}$**, with a sterically encumbered zinc porphyrin core, formed a weak gel in C_6H_6 whose absorption spectrum (Figure 2 a; red curve) was similar to that of non-aggregated **G3/0$_{ester}$** (Figure 2 a; green curve).

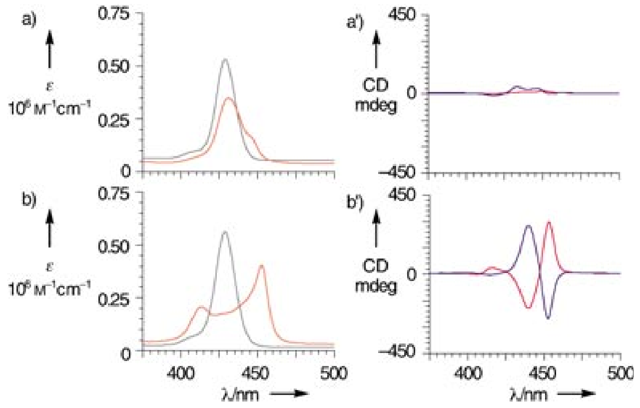

Figure 2. Electronic absorption spectra of solutions (5 mM) of **G3/*n*$_{acid}$** ($n = 0$, 1; red curves) and **G3/*n*$_{ester}$** ($n = 0$, 1; green curves) at 25 °C in C_6H_6; a) **G3/0$_{acid}$** and **G3/0$_{ester}$**, b) **G3/1$_{acid}$** and **G3/1$_{ester}$**. CD spectra of thin films of **G3/*n*$_{acid}$** ($n = 0$, 1) prepared by spin-coating in the clockwise (red curves) and counterclockwise (blue curves) directions are also shown; a′) **G3/0$_{acid}$**, b′) **G3/1$_{acid}$**.

In the course of the above study we noticed that *J*-aggregated **G2/*n*$_{acid}$** ($n = 0$–2) gave birefringent films when cast from their $CHCl_3$ solutions on to glass plates. Spin-coating of these solutions also resulted in the formation of birefringent films, which showed the presence of rodlike crystalline particles by polarized microscopy (Figure 3 a–c). The particles from **G2/0$_{acid}$** were smaller than those from the other two compounds. Quite interestingly, these films were optically active, although their solutions were silent in circular dichroism (CD) spectroscopy. We also found that the spin-coated films displayed a chirality dominance in the statistical distributions that was dependent on the "spinning direction", whereas the cast films did not show any dominance in chirality. For example, when a solution of **G2/2$_{acid}$** in $CHCl_3$ (5 mM) was spin-coated in a clockwise direction at 6000 rpm, the resulting film displayed intense CD bands at 413, 440, and 453 nm with positive, negative, and positive signs, respectively (Figure 1 c′; red curve). On the other hand, spin-coating of the same solution in a counterclockwise direction resulted in the appearance of a mirror-image CD spectrum (Figure 1 c′; blue curve). The intensities of the CD bands hardly changed when observed by rotating the samples along an axis perpendicular to the substrate surface,[8] thus indicating a negligibly small contamination with linear dichroism. Furthermore, we prepared 10 samples for each spinning direction and confirmed a

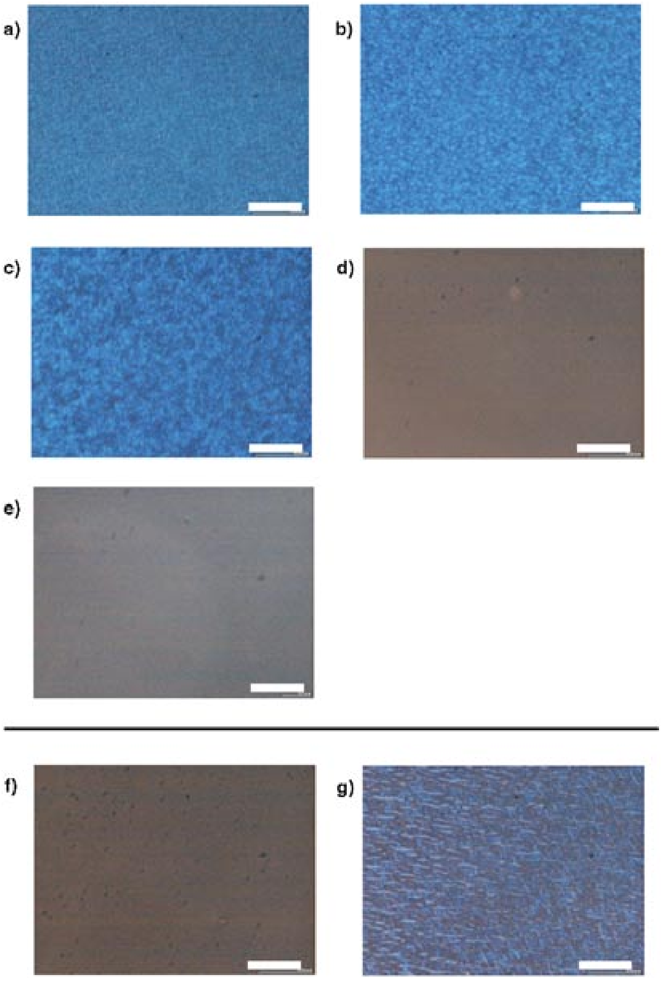

Figure 3. Polarized-light micrographs of spin-coated films from solutions of **G*m*/*n*$_{acid}$** ($m = 2$, 3, $n = 0$–2) in $CHCl_3$ and solutions of **G3/*n*$_{acid}$** ($n = 0$, 1) in C_6H_6: a) **G2/0$_{acid}$**, b) **G2/1$_{acid}$**, c) **G2/2$_{acid}$**, d) **G3/0$_{acid}$**, e) **G3/1$_{acid}$**, f) **G3/0$_{acid}$**, g) **G3/1$_{acid}$**; scale bar, 50 μm.

complete dominance of the emerging chirality sense.[8] Such a spinning direction dependent chirality dominance was also observed for spin-coated films of *J*-aggregated $\mathbf{G2/1_{acid}}$ (Figure 1b′). As already described, the *J*-aggregates of $\mathbf{G2/1_{acid}}$ and $\mathbf{G2/2_{acid}}$ both involve a short, oblique slip of the π-stacked zinc porphyrin units (red curves in Figure 1b and c, respectively). In sharp contrast, *J*-aggregated $\mathbf{G2/0_{acid}}$, which is proposed to involve a long, non-oblique slip of the zinc porphyrin π stacks (Figure 1a; red curve), gave a spin-coated film that exhibited negligibly weak CD bands (Figure 1a′) in the visible region. Similar weak CD bands resulted when nondendritic $\mathbf{G0_{C18}/1_{acid}}$, which is *J*-aggregated in $CHCl_3$ (Figure 1f), was spin-coated (Figure 1f′). These observations indicate the importance of spatial design around the hydrogen-bonded zinc porphyrin chromophores for the emergence of chirality on spin-coating.

One-generation higher $\mathbf{G3/0_{acid}}$, which is not associated through π interactions in $CHCl_3$ (Figure 1d) or even in C_6H_6 (Figure 2a), gave neither birefringent (Figure 3d, f) nor optically active films (Figure 1d′, Figure 2a′) on spin-coating. A nonbirefringent, optically inactive film (Figure 3e, Figure 1e′) also resulted when non-assembled $\mathbf{G3/1_{acid}}$ in $CHCl_3$ (Figure 1e) was spin-coated. In contrast, spin-coating of a solution of *J*-aggregated $\mathbf{G3/1_{acid}}$ in C_6H_6 (Figure 2b) resulted in the formation of a birefringent, optically active film (Figure 3g, Figure 2b′) that exhibited a spinning direction dependent CD response. On the other hand, non-assembled ester versions such as $\mathbf{G\mathit{m}/\mathit{n}_{ester}}$ ($m = 2, 3, n = 0$–2) and $\mathbf{G0_{C18}/1_{ester}}$ (Figure 1a–f; green curves) gave CD-silent films on spin-coating, as expected.

Figure 4 shows a schematic representation of the suggested *J*-aggregated 2D sheet. This is composed of an offset stacking of hydrogen-bonded dendritic zinc porphyrin polymers (Scheme 2). A helical *J*-aggregate structure, proposed for the precedent examples,[5b,c] seems unlikely in solutions, because of a large steric repulsion between the dendritic wedges, along with the one-dimensionality of the backbone polymers. However, such 2D molecular sheets, when transferred to the solid state, are known to role up to form coiled architectures.[4,10] If this happens to the *J*-aggregated 2D sheet, the zinc porphyrin units are forced to adopt a twisted (chiral) geometry relative to one another, and the assembly can eventually be optically active when the parity of chirality is broken. On the other hand, when a large rotational sheer force is applied to this roll-up event by spin-coating, either a right-handed or left-handed helical coil, depending on the spinning direction, may be selected. In other words, the spin-coated films can chiroptically memorize the macroscopic spinning direction. We found that the chiroptical memory thus fixed is thermally stable. For example, the spin-coated film of *J*-aggregated $\mathbf{G2/2_{acid}}$ still preserved its optically activity when heated at 200 °C for five minutes. Further heating the film up to 260 °C resulted in it losing its birefringence and becoming optically inactive.

In summary, we have demonstrated that spin-coating of hydrogen-bonded dendritic zinc porphyrin *J*-aggregates gives optically active films, where either of the two enantiomeric forms is selected by the spinning direction. This is the first successful example of the transformation of a macroscopic spinning chirality into a stable supramolecular chirality in the solid state. Extension of this finding to other self-assembling systems and application of the resulting optically active materials to absolute asymmetric synthesis and chiral separation are the challenging subjects worthy of further investigation.

Received: July 26, 2004

Keywords: chirality · dendrimers · *J*-aggregate · porphyrinoids · self-assembly

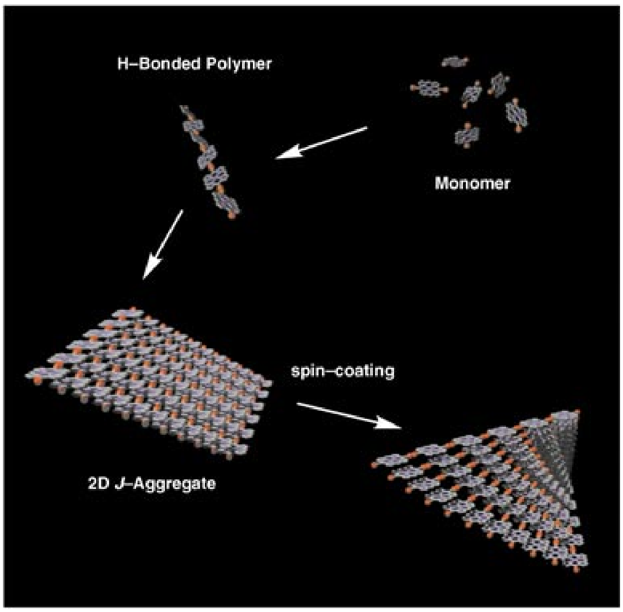

Figure 4. A proposed mechanism for the formation of a chiral zinc porphyrin *J*-aggregate.

---

[1] J. Jacques, A. Collet, S. H. Wilen, *Enantiomers, Racemates, Resolutions*, Wiley, New York, **1998**.

[2] a) D. K. Kondepudi, R. J. Kaufman, N. Singh, *Science* **1990**, *250*, 975–976; b) D. K. Kondepudi, K. L. Bullock, J. A. Digits, J. K. Hall, J. M. Miller, *J. Am. Chem. Soc.* **1993**, *115*, 10211–10216; c) D. K. Kondepudi, J. Laudadio, K. Asakura, *J. Am. Chem. Soc.* **1999**, *121*, 1448–1451.

[3] D. R. Link, G. Natale, R. Shao, J. E. Maclennan, N. A. Clark, E. Körblava, D. M. Walba, *Science* **1997**, *278*, 1924–1927.

[4] X. Huang, C. Li. S. Jiang, X. Wang, B. Zhang, M. Liu, *J. Am. Chem. Soc.* **2004**, *126*, 1322–1323.

[5] a) U. De Rossi, S. Dähne, S. C. J. Meskers, H. P. J. M. Dekkers, *Angew. Chem.* **1996**, *108*, 827–830; *Angew. Chem. Int. Ed. Engl.* **1996**, *35*, 760–763; b) O. Ohno, Y. Kaizu, H. Kobayashi, *J. Chem. Phys.* **1993**, *99*, 4128–4139; c) J. M. Ribó, J. Crusats, F. Sagues, J. M. Claret, R. Ruvires, *Science* **2001**, *292*, 2063–2066.

[6] a) C. Halvorson, A. Hays, B. Kraabel, R. Wu, F. Wudl, A. J. Heeger, *Science* **1994**, *265*, 1215–1216; b) H. S. Nalwa, *Adv. Mater.* **1993**, *5*, 341–358; c) K. Misawa, T. Kobayashi, *J. Chem. Phys.* **1999**, *110*, 5844–5850.

[7] a) S. Okada, H. Segawa, *J. Am. Chem. Soc.* **2003**, *125*, 2792–2796; b) M. Shirakawa, S. Kawano, N. Fujita, K. Sada, S. Shinkai, *J. Org. Chem.* **2003**, *68*, 5037–5044.

[8] See Supporting Information.

[9] J.-H. Furhop, C. Demoulin, C. Boettcher, J. König, U. Siggel, *J. Am. Chem. Soc.* **1992**, *114*, 4159 – 4165.

[10] a) J. M. Schnur, *Science* **1993**, *262*, 1669 – 1676; b) R. Oda, I. Huc, M. Schmutz, S. J. Candau, F. C. MacKintosh, *Nature* **1999**, *399*, 566 – 569; c) E. D. Sone, E. R. Zubarev, S. I. Stupp, *Angew. Chem.* **2002**, *114*, 1781 – 1785; *Angew. Chem. Int. Ed.* **2002**, *41*, 1706 – 1709; d) J. P. Hill, W. Jin, A. Kosaka, T. Fukushima, H. Ichihara, T. Shimomura, K. Ito, T. Hashizume, N. Ishii, T. Aida, *Science* **2004**, *304*, 1481 – 1483.